Journal of Fluorescence, Vol. 4, No. 3, 1994

Study of L-Tryptophan Corepressor Binding to Mutated *E. coli* Tryptophan Repressor Proteins by Optically Detected Triplet-State Magnetic Resonance

Laura E. Burns[1] and August H. Maki[1,2]

Received December 8, 1993; accepted March 1, 1994

Phosphorescence and optically detected magnetic resonance (ODMR) measurements have been carried out on the tryptophan (Trp) residues of *Escherichia coli* Trp repressor protein (W Rep) and its two single Trp-containing mutants, W19F and W99F. The enhanced resolution afforded by the W19F and W99F mutants allowed us to characterize the triplet state of bound L-Trp corepressor using phosphorescence wavelength-selected ODMR spectroscopy. We find that at 77 K the 0,0 band peak wavelength of L-Trp is shifted from 405.5 nm in the aqueous solvent to ca. 410 nm when bound to the corepressor binding site. This red shift of the phosphorescence along with a corresponding increase in the zero-field splitting E value and narrowing of the ODMR linewidth characterize a binding site that is less polar, as well as more polarizable and homogeneous, than the aqueous solvent. This conclusion is in agreement with the X-ray crystallographic structure of the holorepressor protein that places the indole chromophore of the bound corepressor in a cleft in which it is sandwiched by the side chains of arginines 54 and 84.

KEY WORDS: L-Tryptophan (L-Trp); Trp corepressor binding; *Escherichia coli* Trp repressor protein; triplet state; magnetic resonance.

INTRODUCTION

The transcription regulatory protein tryptophan repressor (W Rep) from *Escherichia coli* binds very specifically in the presence of the corepressor L-tryptophan (L-Trp) to the trp EDCBA operon as well as to the aro H and trp R operons [1–4]. The regulation of the operons is through a negative feedback loop; an increase in the concentration of free L-Trp results in the noncooperative binding of two L-Trp residues per aporepressor dimer (K_D,ca. 10^{-5} M), forming the active repressor [5–8]. This readily available regulatory protein has been studied extensively by biochemical as well as biophysical methods and is of interest as a general model for other regulatory proteins [9–11]. The crystal structures of the aporepressor, the functional repressor, and the W Rep bound to the trp EDCBA operator sequence also have been reported [12–15]. W Rep is a dimeric protein consisting of two identical subunits, each 108 amino acids long, that are related by a screw triad [5, 12, 13]. The two monomers are predominantly (72%) α-helical in structure, containing six α-helixes per monomer [12]. Helixes A and B are separated from helixes D, E, and F by about five turns of helix C. Binding of a corepressor, L-Trp, induces changes in the C and D helixes, but helixes A, B, E, and F appear to be indifferent to the binding of L-Trp corepressor [13]. Very large blue shifts in the W Rep room temperature fluorescence upon binding L-Trp support the characterization of the binding site as one of relatively low polarity [6]. X-Ray crystallography re-

[1] Department of Chemistry, University of California, Davis, Davis, California 95616.

[2] To whom correspondence should be addressed.

1053-0509/94/0900-0217$07.00/0

veals that the corepressor binding site resembles a "sandwich" with Arg 84 and the Cα of Gly 85 forming the top and Arg 54 completing the bottom [8,13]. The α-amino group of L-Trp forms essential hydrogen bonds to carboxyl oxygens of the B helix, while the carboxyl group greatly enhances corepressor binding but was found to be not essential [16]. The presumed role of bound L-Trp is to induce a conformational change in the aporepressor such that the reading heads of the dimer can penetrate two successive grooves of the operon [17]. Bound L-Trp, however, apparently does not lock the repressor into a single conformation corresponding to the trp EDCBA operon but perhaps leaves it sufficiently flexible to regulate the other operons as well [15].

The aporepressor contains two Trp residues per monomer at positions 19 and 99 [13]. Trp 19 residues in the A helix and Trp 99 is found in the F helix. The two Trp residues are separated by a distance of 17.6 Å. According to the crystal structure [13] Trp 19 is buried at the interface of the two subunits, while Trp 99 is partially solvent exposed. Two Trp sites with differing solvent exposure also have been distinguished using fluorescence quenching with iodide and acrylamide [18], low-temperature phosphorescence, and optically detected magnetic resonance (ODMR) [18], as well as by NMR spin-lattice relaxation times [19].

The optical emission spectrum of the Trp residue is often used as a reporter yielding information on interactions and events within its realm. Unfortunately, the inhomogeneously broadened structure of the room-temperature Trp fluorescence emission often averages the spectroscopic properties of multiple Trp residues. This appears to be the case for native W Rep [6]. The addition of a third variety of Trp, the corepressor L-Trp, only obscures further the individual Trp properties. As with fluorescence, the phosphorescence emission of multiple Trp chromophores frequently exhibits only a single origin. There are a number of cases, however, where individual Trp residues within a protein molecule exhibit resolved phosphorescence emission spectra [20–23]. In some situations of unresolved phosphorescence emission from two or more Trp residues, a technique of monitoring the ODMR frequency as a function of 0,0 band emission wavelength using narrow-bandpass conditions has been used successfully to distinguish multiple Trp sites [24–27].

The work presented here uses both native and single-point mutants of W Rep in an effort to identify and characterize the triplet-state properties of the intrinsic Trp chromophores and of L-Trp bound to the corepressor binding site. The single-point mutants W19F and W99F, obtained from site-directed oligonucleotide mutagenesis, offer a unique opportunity to examine the triplet state of each chromophore in the absence of interfering emissions.

ODMR of the lowest excited triplet state is a sensitive technique that exploits the more energetic and more readily detected optical photons to monitor the lower-energy microwave transitions between the sublevels of the triplet state. Even in a zero external magnetic field, the magnetic dipole–dipole interactions of the unpaired electrons remove the degeneracy of the triplet sublevels. Spin-lattice relaxation, which is rapid at 77 K, generally is quenched at temperatures below 4.2 K, leaving the sublevel populations effectively decoupled. Resonant microwaves swept slowly through a triplet-state magnetic resonance transition can produce detectable changes in the steady-state phosphorescence if at least one of the coupled sublevels emits photons. Specifically, to observe phosphorescence-detected slow-passage ODMR signals, the coupled sublevels must have differing quantum yields and steady-state populations. Detailed descriptions of ODMR methods with biological applications have been published [28,29]. The energy splittings of the triplet sublevels can be modeled as a perturbation caused by the magnetic dipole–dipole interactions of the unpaired electrons. Two parameters, D and E, are required to express the energy splittings of the triplet sublevels. These zero-field splitting (zfs) parameters are related to the spatial distribution of the two unpaired electrons of the triplet state by the relations:

$$D = \frac{3}{4} g^2\beta^2 \left\langle \frac{r_{12}^2 - 3z_{12}^2}{r12^5} \right\rangle_{avg}$$

$$E = \frac{3}{4} g^2\beta^2 \left\langle \frac{y_{12}^2 - x_{12}^2}{r_{12}^5} \right\rangle_{avg}$$

The term β is the Bohr magneton and g is the electron g-factor. The quantities x_{12}, y_{12} and z_{12} are the projections of the interelectron distance, r_{12}, along the x, y, and z principal magnetic axes, respectively. The zfs are influenced by environmental perturbations that affect the interelectron coordinates. The principal magnetic axes of L-Trp and an energy level diagram of its zfs are given in Fig. 1.

In this paper we employ phosphorescence and ODMR spectroscopy to characterize initially the microenvironments of the intrinsic Trp residues 19 and 99. The use of the single-Trp mutants, W19F and W99F, provides sufficient resolution for characterization of the bound L-Trp corepressor, in addition, using phosphorescence-detected ODMR spectroscopy.

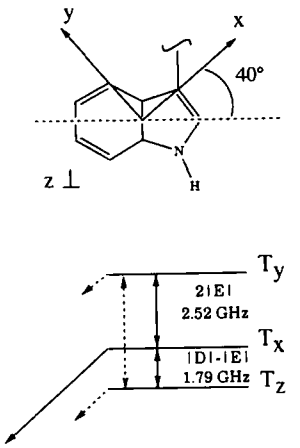

Fig. 1. Principal spin axis system for the triplet state of the Trp chromophore. The solid arrow indicates a primarily radiative depopulating of the associated sublevel, while the dashed arrows represent nonradiative deactivation. The zero-field splittings of the magnetic sublevels of Trp are given in terms of the *D* and *E* parameters. Double-headed solid arrows are the normally observed ODMR transitions when monitoring phosphorescence, while the transition indicated by the dashed double-headed arrow is not observed; the ODMR frequencies were measured for L-Trp in an aqueous ethylene glycol glass [43,44].

MATERIALS AND METHODS

W Rep and the single-point mutants, W19F and W99F, were received in 70% ammonium sulfate and exchanged into a 0.1 *M* potassium phosphate buffer (pH = 7.5, 0.2 *M* KCl, 1 m*M* EDTA) with a final concentration of about 200 μ*M*. The proteins were a generous gift from Prof. Maurice Eftink. Ethylene glycol (Fluka, puriss) was added (40%, v/v) as a cryosolvent to quench spin-lattice relaxation. L-Trp, obtained from Fluka, was used as received. Samples were pipetted into a suprasil quartz sample tube (1-mm i.d.) and suspended in a microwave slow-wave copper helix terminating a coaxial transmission line. The sample was then placed in a Janis, Inc. (Model 8DT), research dewar equipped with optical ports and submerged in either liquid N_2 or liquid He according to the experiment. Temperatures below 4.2 K were obtained by pumping on the liquid He. Exciting light was provided by a 100-W mercury arc lamp passed through a 12-cm $NiSO_4$ solution IR filter (500 g/L). The sample excitation was centered at 295 nm and was selected by a 10-cm monochromator (Instruments SA, Model H-10) with a 16-nm bandpass. Emitted light was collected at a right angle to the excitation, passed through a WG 345-2 glass filter, a 1-m monochromator (Mc Pherson, Inc., Model 2051), and detected by a photomultiplier tube cooled to −5°C (TE-104RF Products for Research). Data were analyzed by either an Everex Step-20 personal computer or a DEC PRO350 microcomputer interfaced to a 1024-channel signal averager (TN1550, Tracor Northern, Inc.). Microwaves were generated using a Hewlett Packard Model 8350B microwave sweep oscillator with a Model 83592A plug in, capable of producing microwave output in the region 0.1–20 GHz.

Phosphorescence lifetime measurements were obtained with optical excitation and collection durations of at least five times the mean lifetime. Phosphorescence decays were deconvoluted using a nonlinear least-squares Marquardt algorithm designed to minimize the chi-square [30]. Goodness of fit was determined through a residuals plot of the data.

Slow-passage optical detection of magnetic resonance (ODMR) was carried out at pumped liquid helium temperatures (~1.2 K). This condition suppresses spin-lattice relaxation and produces a state of spin alignment in the triplet sublevels of Trp when it is in the presence of a cryosolvent such as ethylene glycol [31,32]. The ODMR apparatus and methods have been described in greater detail previously [33]. For consistency, all W Rep samples were prepared with a cryosolvent content of 40% by volume. Typical scans were obtained with a 36-s sweep time. A rotating sector with a dead time of about 800 μs was used to eliminate scattering and fluorescence emission.

RESULTS AND DISCUSSION

Triplet-State Characteristics of Trp Aporepressor. A detailed analysis of the fluorescence and phosphorescence characteristics of the Trp chromophores of apo W Rep has been published previously [18]. For comparative purposes some details of their low-temperature phosphorescence and ODMR are included here. The low-temperature triplet-state characteristics of the two intrinsic Trp residues (tryptophans 19 and 99) of the aporepressor were determined using the native W Rep and the two point mutants, W99F and W19F. Phenylalanine makes no contribution to the phosphorescence or ODMR under the conditions of our experiment.

Phosphorescence spectra of the Trp residues in all three apo W Rep samples are shown in Fig. 2. The phosphorescence emissions from the two Trp chromophores of the native W Rep are clearly resolved in Fig. 2A into two narrow individual 0,0 bands that are centered at 407.5 and 414.9 nm (FWHH = 4.0 nm). Weak tyrosine phosphorescence is found to the blue of Trp with an

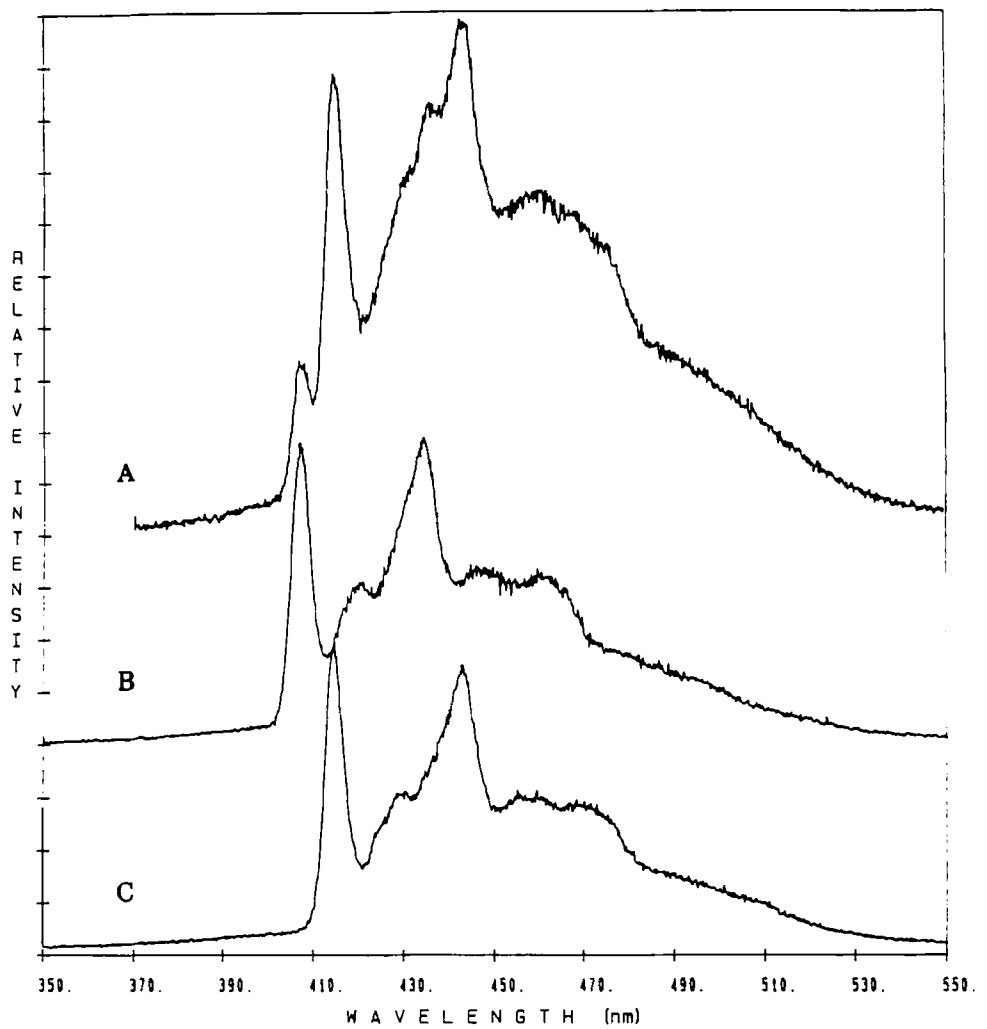

Fig. 2. Phosphorescence spectra of native W Rep (A) and the single-point mutants W99F (B) and W19F (C). Samples are in 0.1 *M* phosphate buffer, 1 m*M* EDTA, 0.2 *M* KCl, pH 7.5. Ethylene glycol is added (40%, v/v) as a cryosolvent. Sample excitation is at 295 nm with a 16-nm bandpass. Emission resolution is 1.5 nm and the sample temperature is 77K. Protein concentrations are ca. 200 μ*M*.

emission maximum at about 400 nm under these conditions. Excitation at wavelengths shorter than 295 nm significantly increases the tyrosine contribution.

The protein samples were frozen at 77 K. Therefore, the local solvent dipole orientations minimize the energy of the ground-state dipole of the indole chromophores. Optical excitation of this frozen system results in a triplet-excited state dipole that is reoriented and consequently no longer stabilized by the rigid solvent dipole geometry [20]. This argument necessitates a blue shift in the phosphorescence spectra of Trp residues that are in primarily polar microenvironments. The hydrophobic core of the protein generally is more polarizable than a solvent exposed environment and the dipole-induced dipole interactions of the protein interior allow for a more extensive redistribution of electron densities, which in turn more adequately stabilize the new orientation of the excited-state dipole moment. Thus, a red shift in the low-temperature phosphorescence such as that seen in the 0,0 band at 414.5 nm is suggested to be the result of stabilization of the excited-state dipole moment by the polarizable interior of the globular protein. The narrower width of the 414.5-nm band also is an indication of the homogeneous nature of the nonpolar protein core [20, 34].

The two single-point mutants, W19F and W99F, allow us to assign the residues corresponding to the two resolved 0,0 bands. W19F, containing only Trp 99, was found to have a simple phosphorescence spectrum exhibiting a single 0,0 band with a FWHH of 3.6 nm at 414.5 nm (Fig. 2C). Both the emission wavelength and the narrow bandwidth indicate that Trp 99 has a polar-

Table I. Phosphorescence 0,0 Band and Lifetimes of W Rep and the Single-Point Mutants W19F and W99F

Sample	0,0 band (nm)[a]	Lifetime (s)[b]	
W Rep	414.9	5.6 (91%)	1.8 (9%)
	407.5	5.9 (77%)	1.1 (23%)
W19F	414.5	6.0 (100%)	
W99F	407.5	6.1 (85%)	2.2 (15%)
L-Trp[c]	405.5	6.9 (100%)	

[a]Excitation was at 295 nm with a 16-nm bandpass.
[b]Lifetimes were obtained at the peak of the indicated 0,0 band in each sample. Excitation and emission times were 36 s and the sample temperature was 77 K.
[c]Dissolved in 40% EG/water (v/v).

izable microenvironment that is homogeneous in nature. Additionally, the energy of the phosphorescence origin is invariant to changes in excitation wavelength (280–295 nm), further confirming the buried nature of the chromophore [35–37]. The observed single phosphorescence 0,0 band of W99F (Fig. 2B) is centered at 407.5 nm (FWHH = 4.2 nm). According to arguments presented earlier by Hershberger *et al.* [34] that are outlined above, these results indicate that Trp 19 is a relatively buried residue that is subject to local polar interactions. It is probably in a somewhat less homogeneous site than residue 99 based on the somewhat broader 0,0 band. Further evidence in support of a limited degree of solvation-site heterogeneity of Trp 19 is a small 0.7-nm red shift in the phosphorescence 0,0 band that occurs upon changing the excitation wavelength from 280 to 295 nm. This is consistent with observations that polar aromatic chromophores in rigid polar solvents experience a red shift in emission when excited to the red edge of the absorption band [35–37]. Although the magnitude of this shift is approximately half that observed for L-Trp in an aqueous glass [35], it is well outside the error of the measurement. Based on a comparison of these phosphorescence spectra in Fig. 2, the local environment of each Trp residue in the native apo W Rep appears to be represented accurately by one of the two point mutants, indicating that replacement of a Trp residue with phenylalanine has little effect on the long-range tertiary structure.

The phosphorescence lifetimes of the native and single-point mutant apo W Reps are given in Table I. They are typical of unperturbed Trp residues at 77 K. The observed short component (1–2 s) is attributed in part to unquenched emission from at least one of the two tyrosine residues present in apo W Rep.

Slow-passage ODMR signals in zero applied magnetic field were obtained by monitoring the change in steady-state phosphorescence intensity as the microwave frequency was swept through the zero-field triplet-state transitions. The optical responses of the triplet state to resonant microwaves were obtained for both the native and the single-point mutants at 1.2 K. The axis convention and corresponding energies D and E for the Trp chromophore are detailed in Fig. 1. Unperturbed Trp has only one strongly radiative sublevel, the T_x sublevel. Thus, only the $2|E|$ resonance (transition coupling T_x and T_y sublevels) and $|D|-|E|$ resonance (transition coupling T_x and T_z sublevels) can be observed using phosphorescence detection. A cryosolvent concentration of 40% (v/v) was required to quench sufficiently spin-lattice relaxation between the triplet sublevels of the short-wavelength 0,0 band. This triplet state, in both the native apo W Rep and the W99F single-point mutant, seemed particularly sensitive to solvent perturbations and exhibited very weak ODMR signals in the absence of sufficient cryosolvent. The $|D|-|E|$ and $2|E|$ triplet-state frequencies and the full width of the ODMR signals at half-height are given in Table II for each sample.

As seen before for the phosphorescence spectra, the correlation of the zero-field splitting parameters between the native W Rep and the appropriate single-point mutant is very good. Trp 19 (0,0 band at 407.5 nm) has, in both instances, higher $|D|-|E|$ and lower $2|E|$ transition frequencies than Trp 99 (0,0 band at 414.9 nm). These values are indicative of a residue subject to a relatively polar environment [34]. The larger linewidths of the Trp 19 ODMR resonances relative to Trp 99 are the result of greater heterogeneity in perturbations influencing the ground and excited triplet state due to a larger distribution of microenvironments. The ODMR linewidth of the $2|E|$ transition of Trp 19 is significantly less than that of L-Trp, indicating that this residue is in a considerably more homogeneous environment than that presented by the external solvent. Conversely, the lower $|D|-|E|$ and higher $2|E|$ energies measured for Trp 99 are characteristic of buried Trp residues and the line widths are comparable to those of other buried Trp residues [34,38]. In contrast with our results based on phosphorescence and ODMR, X-ray crystallography [13,14,39] and fluorescence quenching studies [18,40] indicate that Trp 99 resides in a somewhat solvent-exposed region of the protein. Possible explanations for this discrepancy are offered below.

Although the triplet-state properties of the individual Trp residues of apo W Rep can be assigned by comparison with the single-point mutants when measurements are made monitoring the 0,0 band maxima, wavelength-dependent ODMR studies of the apo-repressors were undertaken in preparation for a

Table II. Zero-Field Triplet-State Splittings of W Rep, W19F, and W99F[a]

Sample	0,0 band (nm)	$\|D\|-\|E\|$ (GHz)	fwhh (MHz)	$2\|E\|$ (GHz)	fwhh (MHz)	$\|D\|$ (GHz)	$\|E\|$ (GHz)
Native	407.5	1.79	100	2.47	170	3.03	1.24
	414.9	1.61	36	2.71	110	2.96	1.36
W19F	414.5	1.60	35	2.72	140	2.96	1.36
W99F	407.5	1.79	100	2.49	180	3.04	1.25
L-Trp[b]	405.5	1.79	100	2.52	260	3.05	1.26
L-Trp–W99F[c]	410	1.72	53	2.63	150	3.03	1.31

[a]The slow-passage zf splittings were obtained by monitoring the optical response to resonant microwaves at the 0,0 phosphorescence band peak with 1.5-nm resolution. All values were obtained at 1.2 K and have been corrected for rapid passage effects. Excitation was at 295 nm with a 16-nm bandpass.

[b]Values for L-Trp in 40% EG/H_2O were obtained in this laboratory.

[c]The phosphorescence 0,0 band peak wavelength and zfs for bound L-Trp are estimated from the study of the wavelength dependence of the L-Trp zfs bound to the two single-point mutants W19F and W99F. See Fig. 5.

comparative study of the active holorepressor, L-Trp bound to W Rep. Wavelength dependences of the ODMR for the native aporepressor, W19F, and W99F were determined by collecting signals at 1.5-nm intervals across the 0,0 bands with a phosphorescence emission resolution of 1.5 nm.

A plot of ODMR frequencies as a function of monitored phosphorescence emission wavelength across the two resolved 0,0 bands of the native aporepresor is presented in Fig. 3. It reveals two easily distinguishable Trp characteristics with an abrupt discontinuity that occurs in the overlap region of the two 0,0 bands. Superposition of the data from wild-type W Rep with the corresponding data from the two mutants W19F and W99F obtained under identical conditions shows remarkable agreement and confirms the excellent reproducibility of the data. The excellent agreement of the data from the native W Rep with those from the single-Trp mutants suggests that mutation of either Trp residue does not affect the environment of the other. Wavelength-dependent ODMR data shown in Fig. 3 for Trp 19 reveal a somewhat greater dependence of the $2|E|$ and $|D|-|E|$ frequencies with monitored emission wavelength than for Trp 99. Wavelength dependence of the zfs is explained by models developed by van Egmond *et al.* [41] and Gradl *et al.* [42] which assume that mixing of higher excited triplet states with the phosphorescent state is induced by solvent electric fields. Calculations lead to a linear dependence of zfs parameters with triplet-state energy for chromophores in contact with a heterogeneous polar environment. In most cases, a buried Trp residue shows much less dependence of the zfs on the monitored emission wavelength than one that is exposed to a polar solvent [21,25,34]. A small wavelength dependence can be noted, however, for Trp 99 of apo W Rep in Fig. 3. Although the phosphorescence origin, ODMR frequencies, band widths, and independence of phosphorescence emission on excitation wavelength of the Trp 99 residue indicate a relatively homogeneous site, the observed wavelength dependence suggests a correlation between the triplet-state electronic energy and its zfs.

Corepressor Binding. The corepressor L-Trp was bound to each form of the aporepressor (native W Rep, W19F, and W99F). The spectra are shown in Fig. 4. Binding of corepressor to native W Rep at a 1:1 (monomer:L-Trp) ratio reveals a phosphorescence spectrum at 77 K (Fig. 4B) that lacks the short-wavelength origin peak of apo W Rep at 407.5 nm (Fig. 4A). Rather, a prominent shoulder is found at about 409.5 nm, while the dominant emission peak remains at 414.9 nm. It was essential that all excess L-Trp be removed when determining the triplet-state characteristics of the bound L-Trp from wavelength dependence studies. Unbound L-Trp is clearly distinguishable by its prominent 0,0 band origin at about 405.5 nm in the W19F 77K phosphorescence spectrum when present at a 1:1 ratio (data not shown). The 0,0 band of unbound L-Trp was eliminated by adding aliquots of W19F until this band was no longer observed. The free L-Trp phosphorescence was no longer detected at a ratio of 1:3.5 (L-Trp to monomer). Under these conditions, corepressor-bound W19F (Fig. 4D) exhibits spectral features similar to those seen for the native W Rep holorepressor (Fig. 4B). The blue shoulder of the W19F complex is less distinct as a result of the reduced concentration of L-Trp in the sample. This observation of a shoulder at about 409.5 nm in the absence of Trp 19 (W19F/L-Trp complex) demonstrates that the emission at 409.5 nm in the native W Rep ho-

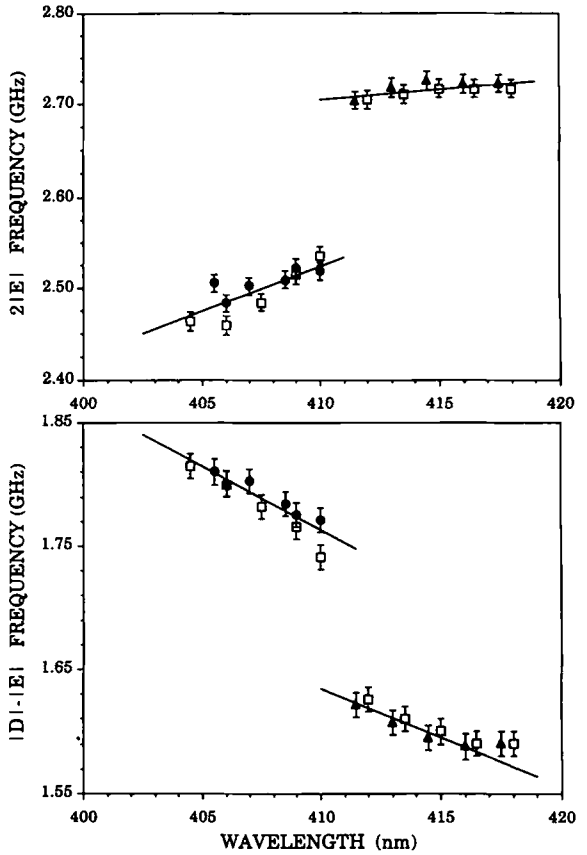

Fig. 3. Comparison of the wavelength dependence of the $|D|-|E|$ and $2|E|$ triplet-state ODMR frequencies as a function of emission wavelength within the 0,0 band for the native W Rep (□) and the single-point mutants W19F (▲) and W99F (●). The temperature is 1.2 K and the emission bandwidth is 1.5 nm. All data have been corrected for rapid-passage effects. Estimated uncertainty of the ODMR frequencies are native W Rep and W19F (±10 MHz) and W99F (±12 MHz).

lorepressor is not a Stokes shift of Trp 19 due to a change in solvent interactions. Rather, it results from the 0,0 band emission of bound L-Trp.

When L-Trp is bound to W99F under the previously discussed conditions (1:3.5), the 0,0 peak undergoes a small red shift to 408.1 nm and a slight broadening of the linewidth is observed (FWHH = 4.6 nm). Upon increasing the L-Trp-to-W99F ratio to 1:1, the 0,0 band maximum is red-shifted further to 410.3 nm and the FWHH increases to 5.4 nm (Fig. 4C). As mentioned above, L-Trp in the buffer system containing 40% ethylene glycol has a 0,0 band at 405.5 nm. Therefore, it is apparent that the red shift of the 0,0 band is caused by an increasing concentration of bound L-Trp rather than the overlap of emission from free L-Trp and W99F.

The plot of the dependence of the $|D|-|E|$ and $2|E|$ triplet-state ODMR frequencies on emission wavelength reveals a pronounced resolution of the bound corepressor, L-Trp. A superposition of the wavelength-dependent zfs parameters of the uncomplexed and complexed forms of the single-point mutants W19F and W99F is given in Fig. 5. These data reveal a region that corresponds to neither of the intrinsic Trp residues of the aporepressor. ODMR resonance frequencies plotted to the far blue and far red correspond to the unperturbed Trp 19 and Trp 99, respectively. Each plot shows a deviation from the intrinsic Trp data as the wavelength moves toward the center of the figure. In the central region of the plot, lines have been drawn that connect data from the corepressor-bound forms of W19F and W99F. These lines represent the triplet-state characteristics of the bound L-Trp corepressor. One can argue further that the 0,0 band peak wavelength of the bound L-Trp corresponds approximately to the median wavelength of the points attributed to bound L-Trp in Fig. 5 (ca. 410 nm). This wavelength matches quite closely the maximum shift in the 0,0 band observed for the active repressor W99F (Fig. 4C) and suggests that Trp 19 emission may be largely quenched by the bound L-Trp corepressor. The triplet-state properties of bound L-Trp corepressor are given in Table II.

The low-temperature triplet-state data discussed above suggest that L-Trp is bound in a site that is less polarizable than that of Trp 99 but is not as polar as that of Trp 19. These ODMR findings corroborate data from UV difference and fluorescence measurements [6], as well as equilibrium dialysis studies [8], indicating that the binding site of L-Trp in the aporepressor provides a polarizable microenvironment. The X-ray crystal structure shows that the planar aromatic indole ring of L-Trp is sandwiched between the hydrocarbon side chains of arg 84 and arg 54 [13].

Differential crystallographic studies of the structural deviations between the aporepressor and the active repressor [13] reveal that only helixes D and E (the DNA binding regions) undergo tertiary structural changes. The remaining extensively interlinked helixes that contain Trps 19 and 99 are quite indifferent to the presence or absence of corepressor, L-Trp. Our data corroborate this observation very nicely for Trp 99. The preservation of structure is particularly evident in the superposition of the wavelength-dependent data of the aporepressor and active W Rep for Trp 99 (Fig. 5). In the wavelength region outside the averaging influence of bound L-Trp, the agreement of the bound and unbound zfs frequencies of Trp 99 indicates essentially no change of the microenvironment. Such conclusions are not readily available

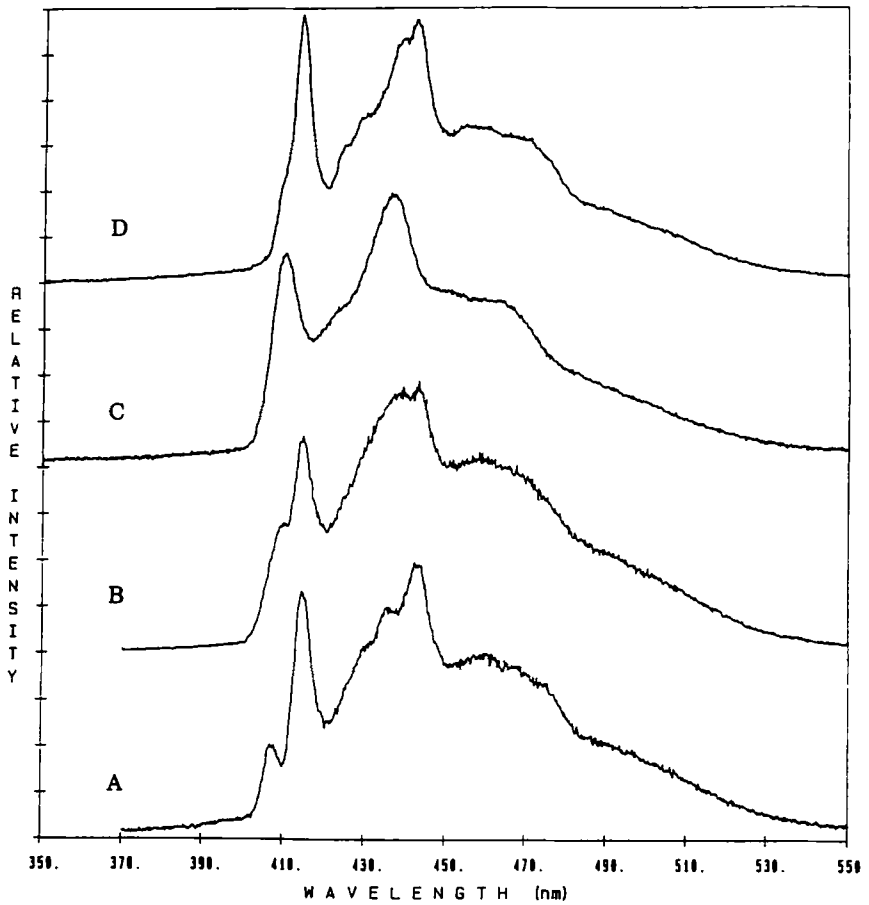

Fig. 4. Low-temperature phosphorescence spectra of single-point mutants with bound L-Trp corepressor: (A) native aporepressor, W Rep; (B) native W Rep + L-Trp; (C) W99F + L-Trp; (D) W19F + L-Trp. Sample conditions are as stated in the legend to Fig. 2. L-Trp is present at a ratio of 1:1 (L-Trp:monomer) except in D, where the ratio is 1:3.5. Experimental temperature is 1.2 K.

for Trp 19, as bound L-Trp appears to quench Trp 19 partially, making a comparison of the microenvironments of Trp 19 in complexed and uncomplexed W Rep difficult.

CONCLUSIONS

This study has employed two single-point mutants, W19F and W99F, to characterize the triplet-state properties of both apo W Rep and the active repressor containing bound L-Trp. From the phosphorescence and ODMR responses we conclude that the two single-point mutants accurately represent the intrinsic properties of the Trp residues in the native W Rep aporepressor. Trp 19 demonstrates the blue-shifted 0,0 band and the characteristic zfs parameters of a residue that is subject to polar interactions. The somewhat broader ODMR and phosphorescence bandwidths and the variability of the 0,0 band wavelength with excitation wavelength suggest that the environment may be partially solvent exposed. Trp 99 was found to exhibit classical triplet-state properties of a residue buried in a hydrophobic environment, although this appears to be an anomaly, as X-ray structures and fluorescence quenching studies provide strong evidence that Trp 99 resides in a partially solvent-exposed environment [5,12,13,18,40]. We think that this discrepancy may result from a structural change in the protein that occurs at a reduced temperature, which may exclude polar solvent from the Trp 99 environment or possibly from a fortuitous arrangement of polar groups in the rigid protein matrix that act to stabilize the excited triplet state relative to the ground state.

The availability of single-Trp mutant proteins, W19F and W99F, allowed the active holorepressor to be characterized. The bound L-Trp corepressor has triplet-state properties that are intermediate between those of Trp 19 and those of Trp 99, exhibiting a phosphores-

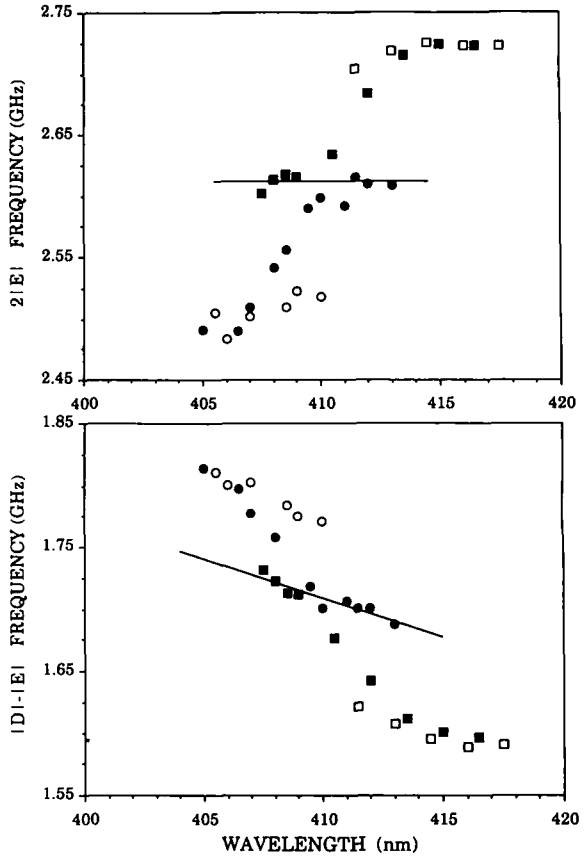

Fig. 5. Slow-passage ODMR frequencies are plotted as a function of 0,0 band emission wavelength across the 0,0 origins of the single-point mutants complexed with L-Trp: W19F + L-Trp (■); W99F + L-Trp (●). For comparison, W19F (□) and W99F (○) aporepressor data are also presented. The straight line through the center of the plot is drawn to indicate the triplet-state properties of bound L-Trp, which is present at a ratio of 1:3.5 (L-Trp:monomer). Slow-passage experimental conditions are described in the legend to Fig. 3.

cence 0,0 band at about 410 nm and zfs intermediate between a residue buried in a hydrophobic environment and one subjected to a polar environment. This assignment is supported by other studies that infer a relatively low-polarity corepressor binding site [6]. We find that the excited state of Trp 19 is quenched to a large extent by the bound L-Trp corepressor.

ACKNOWLEDGMENTS

We thank Professor Maurice Eftink for samples of W Rep and the mutant proteins W19F and W99F. This research was supported by National Institutes of Health Grant ES-02662.

REFERENCES

1. J. K. Rose, C. L. Squires, C. Yanofsky, H.-L. Yang, and G. Zubay (1973) *Nature New Biol.* **245,** 133–137.
2. R. P. Gunsalus and C. Yanofsky (1980) *Proc. Natl. Acad. Sci. USA* **77,** 7117–7121.
3. G. Zurawski, R. P. Gunsalus, K. D. Brown, and C. Yanofsky (1981) *J. Mol. Biol.* **145,** 47–73.
4. R. L. Kelly and C. Yanofsky (1982) *Proc. Natl. Acad. Sci. USA* **79,** 3120–3124.
5. A. Joachimiak, R. L. Kelly, R. P. Gunsalus, C. Yanofsky, and P. B. Sigler (1983) *Proc. Natl. Acad. Sci. USA* **80,** 668–672.
6. A. N. Lane (1985) *Eur. J. Biochem.* **157,** 405–413.
7. D. N. Arvidson, C. Bruce, and R. P. Gunsalus (1986) *J. Biol. Chem.* **261,** 238–243.
8. R. Q. Marmorstein, A. Joachimiak, M. Sprinzl, and P. B. Sigler (1987) *J. Biol. Chem.* **262,** 4922–4927.
9. I. P. Crawford and G. V. Stauffer (1980) *Annu. Rev. Biochem.* **49,** 163–195.
10. T. Platt (1980) in J. H. Miller and W. S. Reznikoff (Eds.), *The Operon,* Ed 2, Cold Spring Harbor Laboratory, Cold Spring Harbor, NY, pp. 263–302.
11. R. L. Sommerville (1983) in K. M. Hermann and R. L. Sommerville (Eds.), *Amino Acid Biosynthesis and Regulation,* Addison–Wesley, Reading, MA, pp. 351–378.
12. R. W. Shevitz, Z. Otwinowski, A. Joachimiak, C. L. Lawson, and P. B. Sigler (1985) *Nature* **317,** 782–786.
13. R.-G. Zhang, A. Joachimiak, C. L. Lawson, R. W. Shevitz, Z. Otwinowski, and P. B. Sigler (1987) *Nature* **327,** 591–597.
14. Z. Otwinowski, R. W. Shevitz, R.-G. Zhang, C. L. Lawson, A. Joachimiak, R. Q. Marmorstein, B. F. Luisi, and P. B. Sigler (1988) *Nature* **335,** 321–329.
15. C. L. Lawson, R.-G. Zhang, R. W. Shevitz, Z. Otwinowski, A. Joachimiak, and P. B. Sigler (1988) *Proteins* **3,** 18–21.
16. R. Q. Marmorstein and P. B. Sigler (1989) *J. Biol. Chem.* **264,** 9146–9154.
17. S. Arnott and D. W. L. Hukins (1972) *Biochem. Biophys. Res. Commun.* **47,** 1504–1509.
18. M. R. Eftink, G. D. Ramsay, L. E. Burns, A. H. Maki, C. J. Mann, C. R. Matthews, and C. A. Ghiron (1993) *Biochemistry* **32,** 9189–9198.
19. A. N. Lane and O. Jardetzky (1985) *Eur. J. Biochem.* **152,** 411–418.
20. R. M. Purkey and W. C. Galley (1970) *Biochemistry* **9,** 3569–3575.
21. J. M. Davis and A. H. Maki (1984) *Biochemistry* **23,** 6249–6256.
22. J. G. Weers and A. H. Maki (1986) *Biochemistry* **25,** 2897–2904.
23. S. Ghosh, L.-H. Zang, and A. H. Maki (1988) *J. Chem. Phys.* **88,** 2769–2775.
24. J.-U. von Schütz, J. Zuclich, and A. H. Maki (1974) *J. Am. Chem. Soc.* **96,** 714–718.
25. S.-Y. Mao and A. H. Maki (1987) *Biochemistry* **26,** 3576–3582.
26. M. I. Khamis, J. R. Casas-Finet, A. H. Maki, J. B. Murphy, and J. W. Chase (1987) *J. Biol Chem.* **262,** 10938–10945.
27. S. Ghosh, L.-H. Zang, and A. H. Maki (1988) *Biochemistry* **27,** 7816–7820.
28. A. H. Maki (1984) in L. J. Berliner and J. Reuben (Eds.), *Biological Magnetic Resonance, Vol. 6,* Plenum, New York, pp. 470–557.
29. A. J. Hoff (1989) in A. J. Hoff (Ed.), *Advanced EPR with Applications in Biology and Biochemistry,* Elsevier, Amsterdam, pp. 633–684.
30. D. W. Marquardt (1963) *J. Soc. Indust. Appl. Math.* **11,** 431–441.
31. S. Ghosh, M. Petrin, and A. H. Maki (1986) *Biophys. J.* **49,** 753–760.

32. H. C. Brenner and V. Kolubayev (1988) *J. Lumin.* **39,** 251–257.
33. A. H. Maki, P. Svejda, and J. R. Huber (1978) *Chem. Phys.* **32,** 369–380.
34. M. V. Hershberger, A. H. Maki, and W. C. Galley (1980) *Biochemistry* **19,** 2204–2209.
35. W. C. Galley and R. M. Purkey (1970) *Proc. Natl. Acad. Sci.* **67,** 1116–1121.
36. K. Itoh and T. Azumi (1973) *Chem. Phys.* **22,** 395–399.
37. K. Itoh and T. Azumi (1975) *J. Chem. Phys.* **62,** 3431–3438.
38. A. H. Maki and T. Co (1976) *Biochemistry* **15,** 1229–1235.
39. C. L. Lawson and P. B. Sigler (1988) *Nature* **333,** 869–871.
40. C. A. Royer, J. A. Gardner, J. M. Beechem, J.-C. Brochon, and K. S. Matthews (1990) *Biophys. J.* **58,** 363–378.
41. J. van Egmond, B. E. Kohler, and I. Y. Chan (1975) *Chem. Phys. Lett.* **34,** 423–426.
42. G. Gradl, J. Friedrich, and B. E. Kohler (1986) *J. Chem. Phys.* **84,** 2079–2083.
43. J. Zuclich (1970) *J. Chem. Phys.* **52,** 3586–3591.
44. J. Zuclich, D. Schweitzer, and A. H. Maki (1973) *Photochem. Photobiol.* **18,** 161–168.